JNK inhibition reduces apoptosis and neovascularization in a murine model of age-related macular degeneration

Hongjun Du[a,b,c,1], Xufang Sun[b,d,1], Monica Guma[e,f,g,1], Jing Luo[b], Hong Ouyang[b], Xiaohui Zhang[b,c], Jing Zeng[b], John Quach[b], Duy H. Nguyen[b], Peter X. Shaw[b], Michael Karin[e,f,2], and Kang Zhang[b,c,h,2]

[a]Department of Ophthalmology, Xijing Hospital, Fourth Military Medical University, Xi'an 710032, China; [b]Institute for Genomic Medicine and Shiley Eye Center, University of California at San Diego, La Jolla, CA 92093; [c]Molecular Medicine Research Center and Department of Ophthalmology, State Key Laboratory of Biotherapy, West China Hospital and Sichuan University, Chengdu 610064, China; [d]Tongji Hospital of Tongji Medical College, Huazhong University of Science and Technology, Wuhan 430030, China; [e]Laboratory of Gene Regulation and Signal Transduction, and Departments of [f]Pharmacology and [g]Pathology, School of Medicine, University of California at San Diego, La Jolla, CA 92093; and [h]Veterans Administration Healthcare System, San Diego, CA, 92161

Contributed by Michael Karin, December 14, 2012 (sent for review August 24, 2012)

Age-related macular degeneration (AMD) is the leading cause of registered blindness among the elderly and affects over 30 million people worldwide. It is well established that oxidative stress, inflammation, and apoptosis play critical roles in pathogenesis of AMD. In advanced wet AMD, although, most of the severe vision loss is due to bleeding and exudation of choroidal neovascularization (CNV), and it is well known that vascular endothelial growth factor (VEGF) plays a pivotal role in the growth of the abnormal blood vessels. VEGF suppression therapy improves visual acuity in AMD patients. However, there are unresolved issues, including safety and cost. Here we show that mice lacking c-Jun N-terminal kinase 1 (JNK1) exhibit decreased inflammation, reduced CNV, lower levels of choroidal VEGF, and impaired choroidal macrophage recruitment in a murine model of wet AMD (laser-induced CNV). Interestingly, we also detected a substantial reduction in choroidal apoptosis of JNK1-deficient mice. Intravitreal injection of a pan-caspase inhibitor reduced neovascularization in the laser-induced CNV model, suggesting that apoptosis plays a role in laser-induced pathological angiogenesis. Intravitreal injection of a specific JNK inhibitor decreased choroidal VEGF expression and reduced pathological CNV. These results suggest that JNK1 plays a key role in linking oxidative stress, inflammation, macrophage recruitment apoptosis, and VEGF production in wet AMD and pharmacological JNK inhibition offers a unique and alternative avenue for prevention and treatment of AMD.

Age-related macular degeneration (AMD) is the leading cause of blindness among elderly patients in developed countries (1, 2). AMD is a progressive degenerative condition with pathological changes in the retinal pigment epithelium (RPE), Bruch's membrane, and the overlying photoreceptors. Early AMD is characterized by the presence of drusen, debris accumulated underneath the retina, without vision loss. Advanced AMD is associated with vision loss and can be divided to geographic atrophy (GA), which is characterized by regional RPE loss and eventual degeneration of overlying photoreceptors, or wet AMD, which is characterized by growth of blood vessels from the choroid through Bruch's membrane toward the retina (choroidal neovascularization, or CNV). These vessels may bleed, resulting in acute loss of central vision. Vascular endothelial growth factor (VEGF) plays a pivotal role in the growth of the abnormal blood vessels in CNV in wet AMD (3).

Although the pathogenesis of AMD is still largely unknown, inflammation, oxidative damage, and RPE senescence have been implicated in this process (4, 5). Oxidative stress is considered by many to be the main initial determinant for various age-related retinal changes. Retinal photoreceptors containing high content of polyunsaturated fatty acids are prone to damage by oxidative stress due to the high oxygen level of the eye and sunlight exposure. The retinal photoreceptors are highly enriched with polyunsaturated fatty acid containing phospholipids and a large amount of oxidized phospholipids (oxPLs) are generated due to oxidative stress caused by stimuli such as sunlight exposure and high oxygen content. Under oxidative stress, these phospholipids can generate a variety of breakdown products to form oxPLs (6), which can be recognized by a natural antibody, TEPC-15 (aka T15). oxPLs on oxidized low density lipoprotein (oxLDL), which can be recognized by T15, have been extensively studied as a marker for systemic inflammation in atherosclerotic lesion development, a condition that shares similarities with drusen development in AMD (7, 8). OxPLs bind to the RPE and macrophages and strongly activate downstream inflammatory cascades (9). oxPLs and their protein adducts can also stimulate RPE cells to express chemoattractant molecules that recruit monocytes into the subretinal space and differentiate into tissue resident macrophages. These oxidatively damaged structures will be further taken up by the macrophages, which consequently release proinflammatory mediators and initiate the inflammation cascade. The accumulation of oxidatively damaged molecules also leads to retinal apoptosis and inflammation. Apoptotic cells, if not rapidly cleared, undergo secondary necrosis and can also stimulate the innate immune system. Thus, oxidative stress and apoptosis are probably the main initial determinants for retinal inflammatory responses (4, 5).

The Jun kinases (JNKs) belong to the mitogen-activated protein kinase (MAPK) family (10). The JNKs, which are encoded by three separate loci, *Jnk1-3*, are activated in response to growth factors, proinflammatory cytokines, microbial components, and a variety of stresses, including oxidative stress (11). The JNKs regulate key cellular processes such as cell proliferation, migration, survival, and cytokine production. Interestingly, it was shown that reactive oxygen species (ROS) cause JNK activation and cell death (12). We also recently showed that JNK1 is a critical factor in hypoxia-induced retinal VEGF production and that it promotes hypoxia-induced pathological angiogenesis (13). Thus, JNK1 might play a key

Author contributions: M.K. and K.Z. designed research; H.D., X.S., M.G., J.L., X.Z., J.Z., J.Q., and P.X.S., performed research; H.D., M.G., H.O., P.X.S., M.K., and K.Z. contributed new reagents/analytic tools; H.D., M.G., D.H.N., P.X.S., M.K., and K.Z. analyzed data; and H.D., X.S., M.G., P.X.S., M.K., and K.Z. wrote the paper.

The authors declare no conflict of interest.

[1]H.D., X.S., and M.G. contributed equally to this work.

[2]To whom correspondence may be addressed. E-mail: karinoffice@ucsd.edu or kang.zhang@gmail.com.

This article contains supporting information online at www.pnas.org/lookup/suppl/doi:10.1073/pnas.1221729110/-/DCSupplemental.

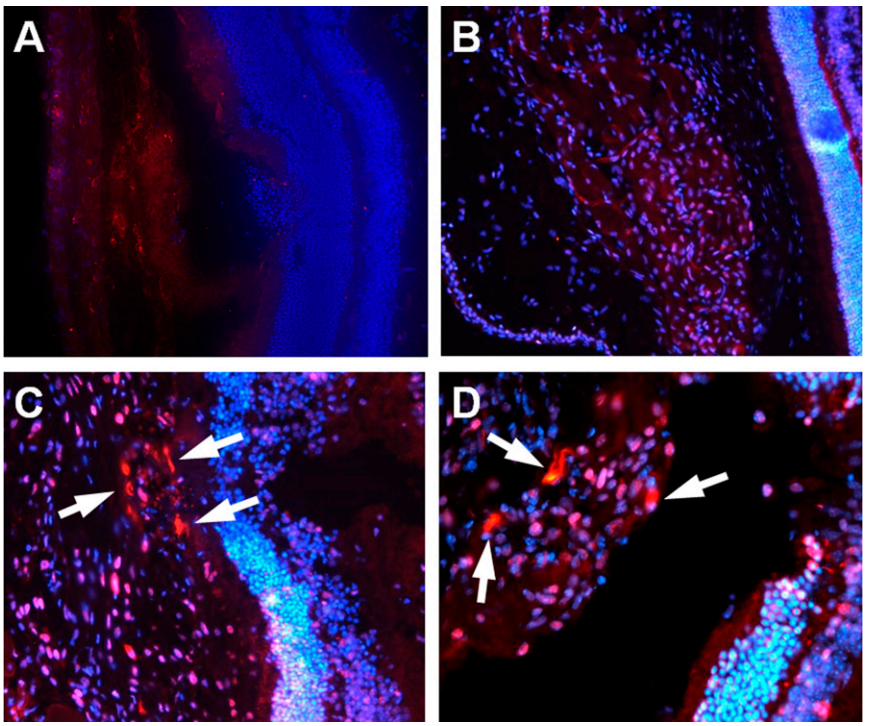

Fig. 1. JNK is activated in a murine model of CNV. Choroids from WT mice, with no intervention (*B*) or subjected to laser-CNV (*C* and *D*, eyes were collected 1 or 3 d after laser treatment, respectively) were stained with a rabbit anti-phospho c-Jun antibody and examined by indirect immunofluorescence (arrows). *A* was a 3D laser CNV section blocked with nonspecific rabbit serum followed by the same anti-rabbit IgG secondary antibody as isotype control. Original magnification, 100×.

role in the development of AMD due to its roles in stress responses and involvement in apoptosis, inflammation, and VEGF production.

Here we show that JNK1 deficiency or JNK inhibition leads to a decrease in apoptosis, VEGF expression, and reduction of CNV in a murine model of wet AMD. Our results indicate that JNK1 plays

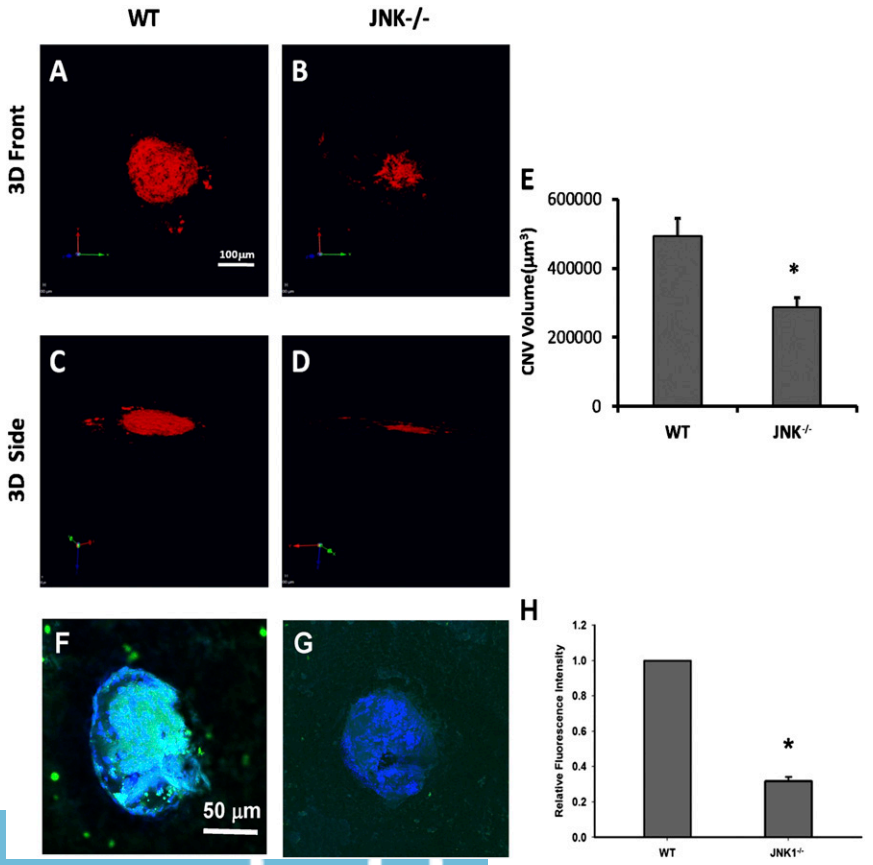

Fig. 2. JNK1 regulates neovascularization and inflammation in a murine model of CNV. Ten days after laser treatment, mice ($n = 20$) were sacrificed and choroidal flat mounts were generated. Alexa-Fluor-conjugated isolectin was used for CNV immunolabeling. Representative images of computer generated 3D front and side views of CNV lesions in choroidal flat mounts from WT (*A* and *C*) and *Jnk1*$^{-/-}$ mice (*B* and *D*) are shown. (*E*) CNV lesion volume was measured by constructed 3D image using Velocity Software (PerkinElmer, Waltham, MA) and expressed as mm^3 (means ± SEM; *$P < 0.01$ vs. WT). (*F* and *G*) The laser-treated CNV flat mounted slides were stained with biotin-T15 antibody followed by FITC-streptavidin showing the reduction of oxPL in CNV lesions in *Jnk1*$^{-/-}$ mice (*G*) compared to that in WT (*F*). Panel *H* shows the relative fluorescent intensity for oxPL epitope. The choroidal flat mounts were originally examined by a Zeiss LSM 510 confocal microscope (Carl Zeiss, Inc.) with 200× magnification. (Scale bars: *A*–*D*, 100 mm; *F* and *G*, 50 mm.)

a critical role in the development of CNV and point to a unique treatment strategy for AMD.

Results

Reduction of CNV and Inflammation in *Jnk1*$^{-/-}$ Mice. To determine if JNK plays a role in the development of CNV, we first examined if JNK is activated in a mouse model of laser-induced CNV (laser-CNV), which is an extensively used animal model for wet AMD. In this model, laser is used to disrupt Bruch's membrane, which allows the underlying choroidal vessels to penetrate and grow into the space underneath the pigment epithelium. Using immunofluorescence, we found that at 1 and 3 d after laser treatment, c-Jun phosphorylation was increased in neovascular tissue (Fig. 1 *C* and *D*, respectively). We next studied the effect of JNK1 deficiency on CNV. CNV was produced in 6–8-wk-old *wild-type* (WT) (Fig. 2*A*) or *Jnk1*$^{-/-}$ (Fig. 2*B*) mice by laser photocoagulation. Ten days after laser treatment, mice were killed and choroidal flat mounts generated and stained with FITC-conjugated isolectin. The mean CNV area at Bruch's membrane was significantly smaller in *Jnk1*$^{-/-}$ mice compared with that in WT controls ($n = 20$) (Fig. 2*C*, $P = 0.0123$). We also assessed oxidative stress and inflammation in CNV by measuring oxLDL, a well-established biomarker for oxidative stress that can be detected with antibody T15. We showed significant reduction of oxPL in CNV lesions in *Jnk1*$^{-/-}$ mice (Fig. 2*E*) compared with that in WT controls (Fig. 2*D*). The relative fluorescence intensity of oxPL staining is 31.6% in CNV of *Jnk1*$^{-/-}$ mice in comparison with WT controls (0.3163 ±0.141 SEM vs. 1.00, $P = 0.0000010798$) (Fig. 2*F*).

Reduction of VEGF and Proinflammatory Cytokines in *Jnk1*$^{-/-}$ Mice. Because VEGF production plays a central role in CNV development in the laser-CNV model and human AMD patients, we examined whether the absence of JNK1 reduces VEGF expression. Choroidal tissues were collected at 3 d after laser administration and placed in medium at 37 °C for 16 h. VEGF levels measured in the supernatants by ELISA showed a significant reduction in the amount of VEGF in choroidal tissue of *Jnk1*$^{-/-}$ mice relative to WT counterparts (Fig. 3*A*). Consistent with this finding, we detected less immunolabeling of VEGF in the CNV in *Jnk1*$^{-/-}$ mice by immunofluorescence (Fig. 3 *B*–*G*). We also assessed other proinflammatory cytokines that are involved in the laser-CNV model, such as tumor necrosis factor (TNF) (14) or IL-6 (15). ELISA of total choroidal protein extracts from laser-CNV mice at day 3 after laser showed a significant reduction in the levels of these cytokines in choroids of *Jnk1*$^{-/-}$ mice (Fig. S1). To assess whether JNK1 controls the expression of these factors transcriptionally, we isolated RNA from choroidal tissues at day 3 after laser and measured mRNA levels. Expressions of VEGF, IL-6, PDGF, and TNF mRNAs were significantly reduced in *Jnk1*$^{-/-}$ mice (Fig. S2).

Reduced Macrophage Infiltration in *Jnk1*$^{-/-}$ Mice. Inflammatory cells, in particular macrophages, have been histologically demonstrated near/within AMD lesions, including areas of Bruch membrane breakdown, RPE atrophy, and CNV. Macrophages in CNV lesions have been shown to secrete proangiogenic factors such as VEGF and proinflammatory cytokines such as TNF. Decreased macrophage influx after laser injury is associated with reduced severity of laser-CNV (16, 17). As migration of different cell types, such as endothelial cells or neutrophils, is associated with JNK activation (18), we studied the presence of macrophages in the choroids after laser-induced injury. We noticed a marked reduction in macrophages (F4/80 positive cells) both by immunofluorescence (Fig. 4 *A*–*F*) and Q-PCR in *Jnk1*$^{-/-}$ mice (Fig. 4*G*). We extracted mRNA from both retinal and choroidal tissues from wild-type and *Jnk1*$^{-/-}$ mice with or without laser-CNV treatment. The qPCR showed that the monocyte chemotactic protein–1 (MCP-1) level is elevated significantly in both retina and choroid after laser-CNV treatment in wild-type mice (Fig. 4*H*). However, only a very moderate increase in MCP-1 mRNA was detected in both retina and choroid in *Jnk1*$^{-/-}$ mice (Fig. 4*I*).

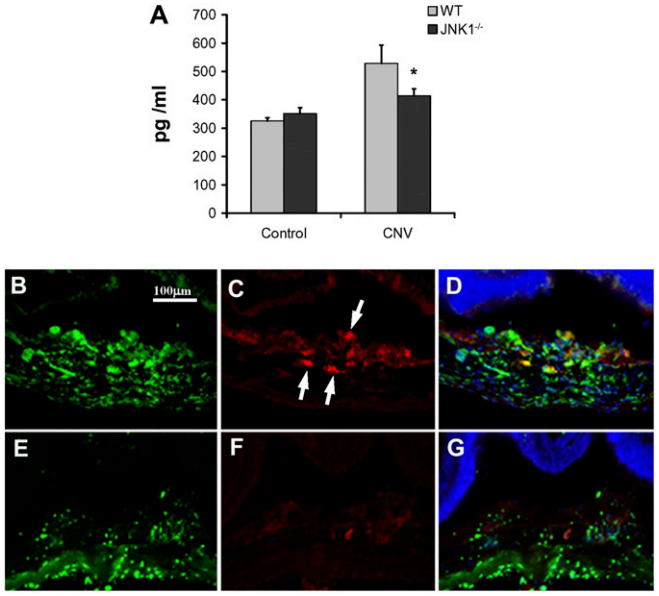

Fig. 3. JNK1 regulates VEGF secretion in a murine model of CNV. (*A*) Choroidal tissues were collected at 3 d after laser administration, placed in 100 μL of RPMI medium supplemented with 10% FCS in 96 wells/ plate, and then kept at 37 °C for 16 h. VEGF levels were analyzed in the supernatants of homogenized tissue by ELISA. Results are averages of two experiments using at least four mice per genotype. Results are expressed as means ± SEM, *$P < 0.05$ vs. WT. (*B*–*G*) Choroidal tissue from either WT (*B*–*D*) or *Jnk1*$^{-/-}$ (*E*–*G*) mice, subjected to laser-CNV and collected 3 d after laser treatment, were stained by immunofluorescence with isolectin (*B* and *E*) and anti-VEGF antibody (*C* and *F*, arrows). *D* and *G* show VEGF, isolectin, and DAPI overlapping staining. Original magnification, 200×.

Reduction of Apoptosis by JNK Deficiency and Pan-Caspase Inhibitor. Although the laser-CNV model mainly mimics the late "wet" phase of AMD, the extent of laser-CNV is significantly lower in antioxidant-treated mice compared with vehicle-treated mice (19), suggesting that this animal model could also mimic some of the pathogenic factors involved in the early "dry" phase of AMD. Oxidative stress can trigger apoptosis, which may activate and recruit macrophages and induce inflammation (4). To examine if apoptosis plays a role in laser-CNV, we tested if a pan-caspase inhibitor benzyloxycarbonyl-Val-Ala-Asp (OMe) fluoromethylketone (Z-VAD-FMK) could reduce neovascularization in this model when injected intravitreally on day 0. We found reduced CNV in mice treated with the pan-caspase inhibitor, suggesting that apoptosis may be one of the triggers of the choroidal inflammation and consequent angiogenesis (Fig. 5*A*). As JNK is activated under oxidative stress and plays a key role in apoptosis (12), we examined the effect of JNK1 deficiency on apoptosis in the choroid 6, 12, and 24 h after laser injury. There was a significant reduction in the number of apoptotic cells visualized by a TUNEL assay in the choroid of *Jnk1*$^{-/-}$ mice (Fig. 5 *B*–*H*).

Intravitreal Injection of a JNK Inhibitor Inhibits CNV. The results shown above suggest that JNK1 may be an excellent target for treating AMD, as its inhibition can reduce apoptosis, macrophage migration, proinflammatory cytokine, and VEGF production. To examine the effect of a JNK inhibitor on CNV, we tested whether D-JNKi (20) injected intravitreally once on day 0 could inhibit neovascularization in the laser-CNV model. Inhibition of CNV by

PHARMACOLOGY

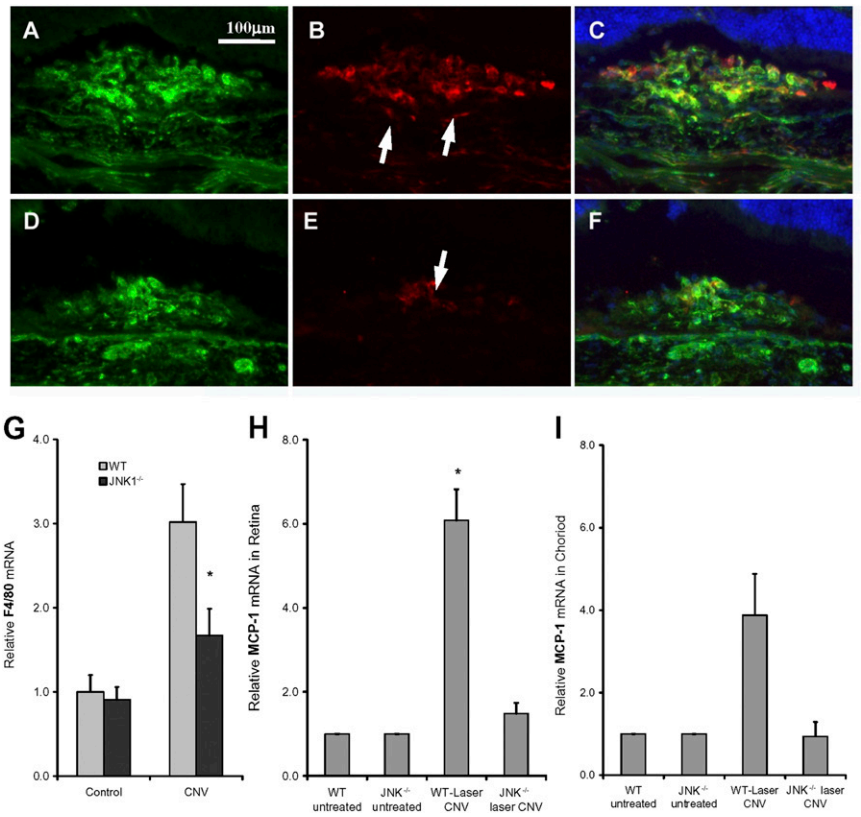

Fig. 4. Reduced macrophage infiltration in *Jnk1*$^{-/-}$ mice. (*A–F*) Choroidal tissue from either WT (*A–C*) or *Jnk1*$^{-/-}$ (*D–F*) mice, subjected to laser-CNV and collected 3 d after laser treatment, were stained by immunofluorescence with isolectin (*A* and *D*) and anti-F4/80 antibody (*B* and *E*, arrows). *C* and *F* show F4/80, isolectin, and DAPI overlapping staining. Original magnification, 200×. (*G*) Choroidal RNA was extracted at day 3 after laser treatment and analyzed by qPCR in triplicates for expression of F4/80 mRNA. mRNA amounts were normalized to 18S rRNA. (*H* and *I*) qPCR showed that the MCP-1 level is elevated significantly in both retina and choroid after laser-CNV treatment in wild-type mice, however, only very moderate increase in MCP-1 level in both retina and choroid was seen in *Jnk1*$^{-/-}$ mice. Results are expressed as means ± SEM, **P* < 0.05 vs. WT.

D-JNKi (Fig. 6 *A* and *B*) was clearly evident 10 d post–laser treatment, where there was reduction of neovascular areas (Fig. 6*C*, $P < 0.01$). D-JNKi treatment also reduced the amount of VEGF and F4/80 positive cells in the neovascular tissue (Figs. S3 and S4).

Discussion

In this report, we show that JNK1 deficiency or total JNK inhibition decreases VEGF expression and reduces CNV in a murine model of wet AMD. The decrease of VEGF in JNK1-deficient mice was expected, as JNK1 regulates VEGF expression under different stimuli such as hypoxia and inflammation (13). However, our data further suggest that JNK1 may also be involved in the initial stages of AMD. Unlike diabetic retinopathy in which the initial triggers for retinal pathogenesis are clear, direct inciting factors of AMD are still largely unknown. Aging, family history, cigarette smoking, systemic inflammation, and genetic predisposition are risk factors for AMD (5). With age, increased oxidative stress exists in retinal/RPE/choroidal tissues, which may result in a number of pathophysiological changes including the formation of oxidized lipids, protein, and DNA; advanced glycation end-products (AGEs); and degeneration of Bruch's membrane, leading to RPE and photoreceptor death. Several mouse models illustrate the capacity of oxidative damage to induce AMD-like pathology (21). Furthermore, one of the known interventions that can reduce AMD progression is consumption of antioxidants (22).

Under normal physiological conditions, cells that undergo apoptosis due to oxidative stress are rapidly cleared by tissue resident phagocytic cells and the proinflammatory response is kept at a minimum. If, however, the apoptotic cells are not rapidly cleared, they undergo secondary necrosis and can generate proinflammatory debris. Late stage apoptotic cells (or secondary necrotic cells) also release damage-associated molecular patterns (DAMP), which can stimulate the innate immune system. Inflammation, such as microglial/macrophage activation, is then induced to trigger tissue repair and remodelling. In AMD, the balance between the stress-induced damage and inflammation-related tissue repair and remodelling is disturbed due to either increased damage or decreased/altered repair/remodelling ability of the immune system (4, 5). Thus, a strategy for targeting apoptosis, for instance, by inhibiting JNK, in this context, might be beneficial.

Apoptosis, however, might play a dual role in the murine laser-CNV model. In this model, which mainly mimics wet AMD, several reports have demonstrated FasL^{+} RPE cells in close proximity to and surrounding Fas^{+} vascular endothelial cells in new vessels (23). This indicates that RPE cells attempt to control the spread of new Fas^{+} vessels as they penetrate Bruch's membrane and are localized beneath the retina. There is also a substantial increase in the incidence and severity of new vessel growth in Fas-deficient and FasL-defective mice, suggesting that apoptosis may control the growth and development of new subretinal vessels that can damage vision (23). However, our data show that inhibiting apoptosis in the first several hours after laser treatment reduced neovascularization, suggesting that apoptosis may be one of the triggers of the choroidal inflammation and consequent angiogenesis in this model. That, together with a recent report that showed a reduction of CNV in antioxidant-treated mice (19), suggests that this model may have some characteristics of dry AMD and treatments that inhibit apoptosis may also be beneficial in some dry AMD patients, in addition to inhibition of other pathways involved in dry AMD (24, 25). Interestingly, JNK is not simply a proapoptotic protein kinase (26). It is activated by a variety of extracellular stimuli as well as by growth factors, only some of which induce apoptosis. In addition, apoptosis can also be induced independent of caspase activation. Therefore, although we showed that the apoptosis was markedly reduced after laser treatment in JNK1-deficient mice, further experiments are needed to study the pro- or anti-apoptotic role of JNK1 in neovascular growth.

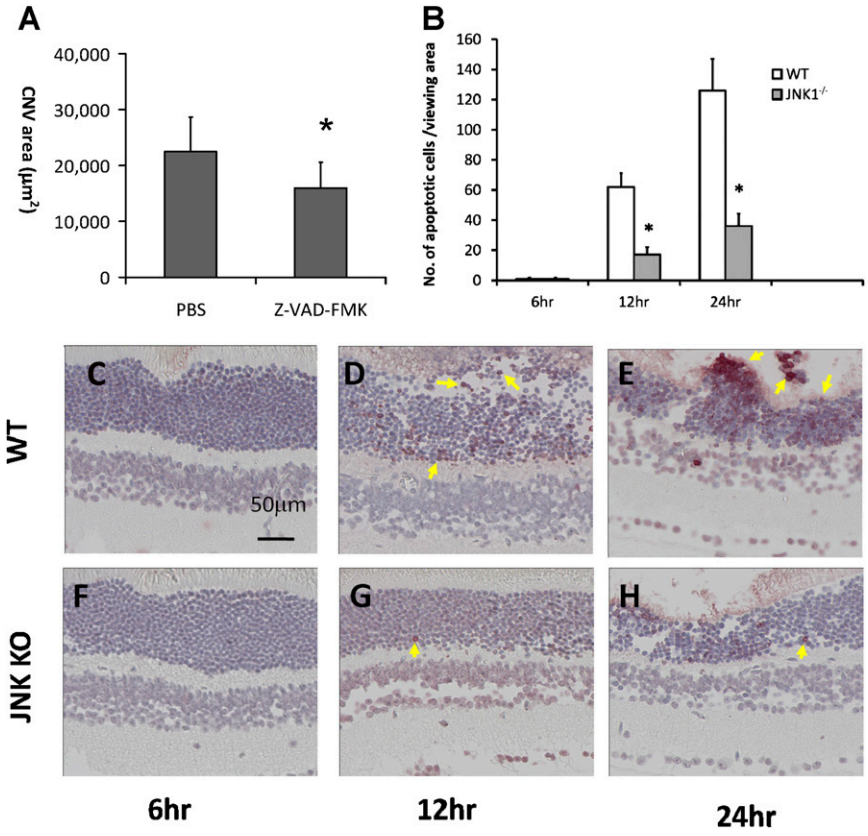

Fig. 5. JNK1 regulates apoptosis in a murine model of CNV. (*A*) WT mice ($n = 10$) were given an intravitreal injection of 1 μL of pan-caspase inhibitor *Z-VAD*-FMK (20 μM) right after laser treatment. An equal volume of PBS was given in the fellow eye as a control. Ten days after laser treatment, mice were killed and choroidal flat mounts generated. FITC-conjugated isolectin was used to immunolabel the CNV. Flat mounts were examined and CNV quantified. Results are expressed by CNV area (μm^2) as means ± SEM, $^*P < 0.01$ vs. PBS. (*B*) The retina of $Jnk1^{-/-}$ and WT control mice were examined for apoptosis by an in situ TUNEL assay with retinal cross-sections obtained 6, 12, and 24 h after laser-CNV treatment. Results are expressed as number of apoptotic cells within the 20× viewing area ($n = 3$, means ± SEM, $^*P < 0.01$ vs. WT). (*C–H*) Representative images of retinal cross-sections of WT control (*C–E*) and $Jnk1^{-/-}$ (*F–H*) mice stained by an in situ TUNEL assay 6, 12, and 24 h after laser-CNV treatment (arrows indicate the positive TUNEL staining). Original magnification, 200×.

The role of macrophages in CNV is also controversial, as it is debated whether macrophages serve an adaptive role to combat CNV or a causative role in inducing CNV (5). For instance, the $Ccl2^{-/-}$ and $Ccr2^{-/-}$ murine models of AMD suggest a protective role for macrophages, in which clearance of deposits by macrophages was proposed (27). This is in contrast to another report that decreased macrophage influx after laser injury to $Ccl2^{-/-}$ mice is associated with reduced laser-CNV (28). There are two subtypes of macrophages, the proinflammatory M1 macrophages and the relatively anti-inflammatory M2 macrophages, which function in scavenging and tissue remodeling (29). Therefore, it is possible that M2 macrophages in early stages of CNV development perform the beneficial, long-term housekeeping role of scavenging deposits such as drusen. In contrast, once inflammation has been triggered, M1 macrophages are recruited and become activated. This may induce and exacerbate the inflammatory response to retinal injury by laser, therefore accelerating CNV development. In this context, inhibiting macrophage migration and activation to inflamed areas would be relevant. Migration of different cell types has been associated with JNK1/2 activation (18). The labile adhesions required for rapid cell migration in response to a variety of stimuli were attributed to the JNK-mediated phosphorylation of paxillin (18). As several chemokines were shown to recruit macrophages in the eye (5), a strategy for targeting the converging intrinsic mechanisms of macrophage migration might be more effective.

In summary, our work shows the importance of interplay among oxidative stress, inflammation, macrophage recruitment, apoptosis, and VEGF production in CNV, in which JNK1 serves as a critical link. And pharmacological JNK inhibition offers a unique and alternative avenue for prevention and treatment of AMD.

Materials and Methods

Mice. $Jnk1^{-/-}$ mice were previously described and were crossbred in the C57BL/6 background (30). C57BL/6 mice were purchased from the Jackson Laboratories. Mice were bred and maintained under standard conditions in the University of California, San Diego animal facility, which is accredited by the American Association for Accreditation of Laboratory Animal Care. All

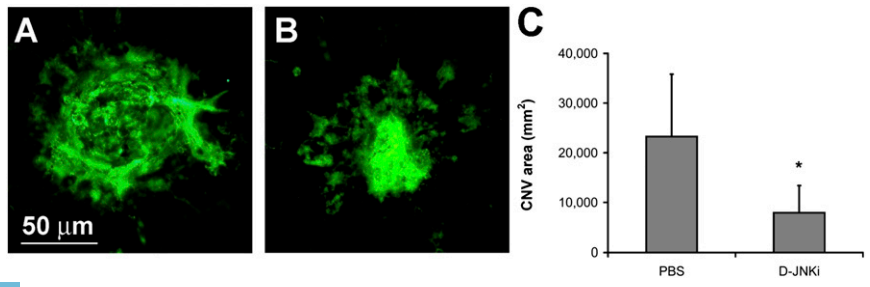

Fig. 6. Intravitreal injection of a JNK inhibitor prevents CNV (*A–C*). WT mice ($n = 10$) were given an intravitreal injection of 1 μL of D-JNKi peptide (2 mM) right after laser treatment. An equal volume of PBS was given by intravitreal injection in the fellow eye as a control. Ten days after laser treatment, mice were killed and choroidal flat mounts generated. FITC-conjugated isolectin was used to immunolabel the CNV. (*A* and *B*) Representative CNV lesions in choroidal flat mounts from PBS and D-JNKi–treated mice. CNV lesion areas were larger in control (*A*) compared with D-JNKi–treated (*B*) mice. Original magnification, 200×. (*C*) Flat mounts were examined and CNV quantified. Results are expressed as means ± SEM, $^*P < 0.01$ vs. PBS.

animal protocols received prior approval by the institutional review board and were conformed to the Association for Research in Vision and Ophthalmology Statement for the Use of Animals in Ophthalmic and Vision Research.

Laser-CNV. All 2–3-mo-old mice were anesthetized with Avertin and their pupils dilated with 1% tropicamide (Alcon). An Iridex OcuLight GL 532 nm laser photocoagulator (Iridex) with slit-lamp delivery system was used to create four burns, three disk diameters from the optic disk at 0300, 0600, 0900, and 1200 hours with the following parameters: 120 mW power, 75 μm spot size, and 0.1 s duration. Production of a bubble at the time of laser treatment, indicating rupture of Bruch's membrane, is an important factor in obtaining CNV; therefore, only burns in which a bubble was produced were included in this study. Twenty burns were generated when the choroids were extracted and homogenized to analyze mRNA and protein content. For pharmacological inhibition experiments, mice were given an intravitreal injection of 1 μL of D-JNKi peptide (20) (concentration of 2 mM) or 1 μL of the pan-caspase inhibitor Z-VAD-FMK (20 μM; Calbiochem) right after laser treatment. An equal volume of PBS was given by intravitreal injection in the fellow eye as a negative control.

Quantification of CNV. Ten days after laser treatment, mice were killed and choroidal flat mounts were generated. FITC-conjugated isolectin (Invitrogen) was used to perform immunolabeling of CNV. Flat mounts were examined using a Zeiss LSM 510 confocal microscope (Carl Zeiss, Inc.) and CNV quantified using ImageJ software (National Institutes of Health) to calculate the area of isolectin positive staining as areas of CNV.

Immunohistochemistry of oxPLs. The laser-CNV–treated eyes were fixed in 4% (vol/vol) paraformaldehyde, and retinas dissected and flat mounted. Immunohistochemistry was performed using the monoclonal anti oxPC mouse IgA antibody T15 (Sigma, 5 μg/mL) followed by FITC-conjugated anti-mouse IgA (Invitrogen) as a secondary antibody. Immunolabeling was examined using a Zeiss LSM 510 confocal microscope (Carl Zeiss, Inc.).

Quantitative-RT-PCR (Q-PCR). RPE/Choroid was collected at 3 d after laser administration. Total RNA was extracted with TRIzol (Invitrogen) and reverse-transcribed with random hexamers and SuperScript II Kit (Invitrogen). Q-PCR was performed with SYBR Green PCR Master Mix Kit (Applied Biosystems). The relative amounts of transcripts were compared with those of 18S mRNA and normalized to untreated samples by the ΔΔCt method. Primer sequences are available upon request.

Cytokine Quantification. Cytokines were analyzed by enzyme-linked immunoabsorbent assay (ELISA) according to the manufacturer's instructions. Choroids were collected at 3 d after laser administration and were homogenized in lysis solution. Protein concentration was measured and IL-1β, TNF, and IL-6 ELISA were performed (R&D Systems, Inc.). To analyze VEGF protein levels, choroidal tissues were collected at 3 d after laser administration, placed in 100 μL of RPMI medium supplemented with 10% (vol/vol) FCS in 96 wells per plate and then kept at 37 °C for 16 h. VEGF levels were analyzed in the supernatants by ELISA (R&D Systems, Inc.).

Histology and TUNEL Assay. Mouse eyes were enucleated and fixed in 4% paraformaldehyde. We obtained and used 10 μm frozen sections for immunofluorescence and TUNEL analysis. For immunofluorescence labeling, frozen sections were first incubated with FITC-conjugated isolectin, and then they were blocked with 3% (wt/vol) BSA and incubated with rabbit antiphospho-S63-c-Jun (Cell Signaling Technology, Inc.), rabbit anti-VEGF (Santa Cruz), or rat anti-F4/80 (AbD Serotec) antibodies. The fluorescent-labeled secondary antibodies were followed and imaged under Zess Observer A1 microscope. The nuclei were stained with DAPI. In situ TUNEL assay was performed using DNA Fragmentation Assay Kit, (Invitrogen).

Statistical Analyses. Data are expressed as mean ± SEM (s.e.m.). The Student *t* test was used to assess statistical significance. All statistical analyses were performed using PRISM version 4.0b (GraphPad Software). A P value < 0.05 was considered statistically significant.

ACKNOWLEDGMENTS. We thank Guy Hughes and members of K.Z. and M.K. laboratories for their assistance and helpful discussions. This work is supported in part from 973 Program Grants 2011CB510200 and 2013CB967504; National Institutes of Health Grants ES00451, ES006376, EY018660, EY021374, EY019270, and EY014428; Superfund Research Program Grant ES010337; and VA Merit Award, the Arthritis Foundation, the King Abdulaziz City for Science and Technology-University of California San Diego Center of Excellence in Nanomedicine, and the Burroughs Wellcome Fund Clinical Scientist Award in Translational Research.

1. Chen Y, Bedell M, Zhang K (2010) Age-related macular degeneration: Genetic and environmental factors of disease. *Mol Interv* 10(5):271–281.
2. Jager RD, Mieler WF, Miller JW (2008) Age-related macular degeneration. *N Engl J Med* 358(24):2606–2617.
3. Bressler SB (2009) Introduction: Understanding the role of angiogenesis and antiangiogenic agents in age-related macular degeneration. *Ophthalmology* 116(10): Suppl):S1–S7.
4. Xu H, Chen M, Forrester JV (2009) Para-inflammation in the aging retina. *Prog Retin Eye Res* 28(5):348–368.
5. Ding X, Patel M, Chan CC (2009) Molecular pathology of age-related macular degeneration. *Prog Retin Eye Res* 28(1):1–18.
6. Shaw PX, et al. (2000) Natural antibodies with the T15 idiotype may act in atherosclerosis, apoptotic clearance, and protective immunity. *J Clin Invest* 105(12): 1731–1740.
7. Mullins RF, Russell SR, Anderson DH, Hageman GS (2000) Drusen associated with aging and age-related macular degeneration contain proteins common to extracellular deposits associated with atherosclerosis, elastosis, amyloidosis, and dense deposit disease. *FASEB J* 14(7):835–846.
8. Curcio CA, Johnson M, Huang JD, Rudolf M (2010) Apolipoprotein B-containing lipoproteins in retinal aging and age-related macular degeneration. *J Lipid Res* 51(3): 451–467.
9. Chou MY, et al. (2008) Oxidation-specific epitopes are important targets of innate immunity. *J Intern Med* 263(5):479–488.
10. Karin M, Gallagher E (2005) From JNK to pay dirt: Jun kinases, their biochemistry, physiology and clinical importance. *IUBMB Life* 57(4-5):283–295.
11. Davis RJ (2000) Signal transduction by the JNK group of MAP kinases. *Cell* 103(2): 239–252.
12. Kamata H, et al. (2005) Reactive oxygen species promote TNFalpha-induced death and sustained JNK activation by inhibiting MAP kinase phosphatases. *Cell* 120(5): 649–661.
13. Guma M, et al. (2009) Genetic and pharmacological inhibition of JNK ameliorates hypoxia-induced retinopathy through interference with VEGF expression. *Proc Natl Acad Sci USA* 106(21):8760–8765.
14. Shi X, et al. (2006) Inhibition of TNF-alpha reduces laser-induced choroidal neovascularization. *Exp Eye Res* 83(6):1325–1334.
15. Izumi-Nagai K, et al. (2007) Interleukin-6 receptor-mediated activation of signal transducer and activator of transcription-3 (STAT3) promotes choroidal neovascularization. *Am J Pathol* 170(6):2149–2158.
16. Espinosa-Heidmann DG, et al. (2003) Macrophage depletion diminishes lesion size and severity in experimental choroidal neovascularization. *Invest Ophthalmol Vis Sci* 44(8):3586–3592.
17. Sakurai E, Anand A, Ambati BK, van Rooijen N, Ambati J (2003) Macrophage depletion inhibits experimental choroidal neovascularization. *Invest Ophthalmol Vis Sci* 44(8):3578–3585.
18. Huang C, Rajfur Z, Borchers C, Schaller MD, Jacobson K (2003) JNK phosphorylates paxillin and regulates cell migration. *Nature* 424(6945):219–223.
19. Hara R, et al. (2010) Suppression of choroidal neovascularization by N-acetyl-cysteine in mice. *Curr Eye Res* 35(11):1012–1020.
20. Borsello T, et al. (2003) A peptide inhibitor of c-Jun N-terminal kinase protects against excitotoxicity and cerebral ischemia. *Nat Med* 9(9):1180–1186.
21. Hollyfield JG, et al. (2008) Oxidative damage-induced inflammation initiates age-related macular degeneration. *Nat Med* 14(2):194–198.
22. Krishnadev N, Meleth AD, Chew EY (2010) Nutritional supplements for age-related macular degeneration. *Curr Opin Ophthalmol* 21(3):184–189.
23. Kaplan HJ, Leibole MA, Tezel T, Ferguson TA (1999) Fas ligand (CD95 ligand) controls angiogenesis beneath the retina. *Nat Med* 5(3):292–297.
24. Zhang K, Zhang L, Weinreb RN (2012) Ophthalmic drug discovery: Novel targets and mechanisms for retinal diseases and glaucoma. *Nat Rev Drug Discov* 11(7):541–559.
25. Dridi S, et al. (2012) ERK1/2 activation is a therapeutic target in age-related macular degeneration. *Proc Natl Acad Sci USA* 109(34):13781–13786.
26. Liu J, Lin A (2005) Role of JNK activation in apoptosis: A double-edged sword. *Cell Res* 15(1):36–42.
27. Ambati J, et al. (2003) An animal model of age-related macular degeneration in senescent Ccl-2- or Ccr-2-deficient mice. *Nat Med* 9(11):1390–1397.
28. Luhmann UF, et al. (2009) The drusenlike phenotype in aging Ccl2-knockout mice is caused by an accelerated accumulation of swollen autofluorescent subretinal macrophages. *Invest Ophthalmol Vis Sci* 50(12):5934–5943.
29. Sica A, Mantovani A (2012) Macrophage plasticity and polarization: in vivo veritas. *J Clin Invest* 122(3):787–795.
30. Sabapathy K, et al. (1999) JNK2 is required for efficient T-cell activation and apoptosis but not for normal lymphocyte development. *Curr Biol* 9(3):116–125.